International Journal for Housing Science and Its Applications
Publish August 5, 2025. Volume 46, Issue 3 Pages 4399-4408

https://doi.org/10.70517/ijhsa463376

Research on power supply meshing model based on quantitative analysis under dynamic change of grid loads

Haiyun An[1,*], Qian Zhou[1], Xiaorong Yu[2], Bingcheng Cen[1] and Yuqi Hou[3]
[1] Research Institute of State Grid Jiangsu Electric Power Co., Ltd., Nanjing, Jiangsu, 211103, China
[2] State Grid Jiangsu Electric Vehicle Service Co., Ltd., Nanjing, Jiangsu, 210004, China
[3] Tianjin University, Tianjin, 300072, China

Corresponding authors: (e-mail: haiyun_229@163.com).

Abstract The continuous expansion of the power supply grid scale and the high proportion of renewable energy access make the dynamic change characteristics of the grid load more and more significant, and the traditional power supply grid division method has been difficult to adapt to the complexity and variability of the power supply operation requirements. In this paper, the research of scientific planning method of power supply grid is carried out. By clarifying the definition of power supply unit, and based on the load transfer mode of the regional scope. Corresponding the planning area to different power supply grids, combined with the load characteristics, the grid planning process of power supply grids is designed. The trend extrapolation method is selected as the load forecasting method within the built-up area with high regional development level. Meanwhile, a gray Verhulst model is established to correct the prediction data and improve the prediction accuracy. After obtaining the load characteristics of the grid, the division of power supply is carried out on the basis of power supply grid division, and the power supply unit division model is constructed. Considering the technical differences between inter-station and intra-station power supply unit division, a technical framework of power supply unit division order and iterative division is proposed. By optimizing the power supply units under dynamic load, the grid division within the power supply area is completed. By using this model to optimize the grid division of power supply in the W area, it is expected that the line insulation rate, the line power supply radius compliance rate and the power supply automation coverage rate will be increased to 100%, which can satisfy the load development demand and power supply reliability in the area.

Index Terms power supply meshing model, grid load forecasting, trend extrapolation, gray Verhulst model

I. Introduction

In the context of the new electricity reform, the distribution side of the market is gradually opening up, and improving the quality of customer service has become an urgent concern for power supply enterprises, and differentiated planning and refined management have been put on the agenda [1]. Distributed renewable energy power generation is developing rapidly, wind and other clean energy distributed power in the distribution network penetration rate is getting higher and higher has become an inevitable trend [2], [3]. Due to the randomness and volatility of distributed power sources, as well as the increasing complexity of distribution grids with multiple flexible and controllable resources makes the active distribution grid operation and control extremely complex, resulting in an increase in the types of distribution grid loads and large differences between each other [4]-[6]. As an example, the real load characteristics of a self-producing PV producer and seller include both fluctuations in the electrical load itself and fluctuations in the PV output [7], [8]. Traditional planning methods do not take into account the variability of this type of load, and it is necessary to carry out finer planning based on the consideration of net load [9].

In order to reduce the control dimension and control difficulty of active distribution network operation and control, the distribution network containing a large number of distributed power sources, flexible loads, energy storage, and other flexible and controllable resources is divided into virtual grids, forming a control pattern with local control within the grid and coordinated interactive control between grids [10]-[13]. Thus, a distribution grid operation and control problem with high complexity and dimension is transformed into multiple relatively simple, and low-dimensional grid partitioned small system operation and control problems [14]-[16]. The grid partitioning of power supply can promote the local consumption of renewable energy sources such as wind power and improve the utilization rate of wind power, and also ensure the necessary quality of power supply through off-grid operation in the event of a fault in the distribution network [17], [18]. Therefore, distribution grid planning methods that consider lean and differentiation are emerging.

In this paper, we first define the regional scope of power supply units within different power supply grids and design the grid planning process based on the dynamic characteristics of grid loads. Secondly, it discusses the steps of trend extrapolation for predicting the loads of supply grids in the built-up area, and the process of residual correction of the predicted data by the gray Verhuslat model. By combining the trend extrapolation method and the gray Verhuslat model, a highly accurate prediction of the dynamic load of the power supply grid is realized. Once again, the power supply area is optimally combined into power supply units, and the power supply unit division model is constructed and the objective function and constraints are clarified. At the same time, considering the differences in the division of power supply units within and between power supply stations, we design the solution sequence and the solution framework of different power supply units, so as to establish the power supply grid division model. Finally, the proposed model is used as an experimental object to train the load forecasting capability of the proposed model, and analyze the effectiveness of the model on the planning of power supply grid division in the W area.

II. Delineation method of power supply grid

II. A.Power supply unit

This paper defines power supply units as electrically independent medium-voltage line power supply areas with moderate load sizes (where different power supply units are electrically connected only through a higher-level power supply substation), e.g., power supply areas involved in a typical 10 kV connection of groups 1-3. The zoning based on the load transfer mode is shown in Figure 1. Each area surrounded by a solid red line represents a power supply unit, which can be categorized into inter-station power supply units, self-loop power supply units and radial power supply units according to the presence or absence of backup substations (hereinafter referred to as backup stations) and medium-voltage backup line channels for the loads within the unit. An inter-station power supply unit is an area where two substations are used as power supply substations as far as possible and the load can be transferred between different power supply stations, e.g. inter-station power supply units ABJ1 and ABJ2 in Fig. 1(a).A self-loop power supply unit is an area where only one substation is used as a power supply substation, and the internal load can be transferred through the different medium-voltage line passages of this substation, e.g. self-loop power supply unit AH11 in Fig. 1(b). AH11 Radial power supply unit is an area where the internal load has only one power supply substation and there is no MV transfer line channel, i.e. a radial line power supply area, e.g. radial power supply unit AS11 in Fig. 1 (b).

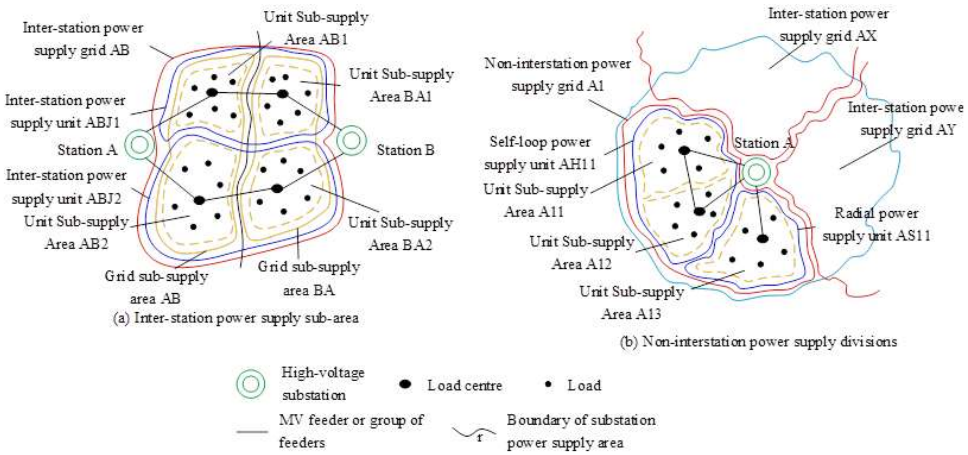

Figure 1: Schematic diagram of area division based on load transfer modes

II. B.Gridded Planning Process Considering Load Characteristics

The grid planning process considering load characteristics is shown in Fig. 2, and the process mainly includes data collection, analysis of the current grid, load forecasting, substation planning, power supply grid division, power consumption unit division, power supply unit division, trunk line planning, branch line planning and corridor planning. Among them, power supply grid delineation, electricity consumption unit delineation and power supply unit delineation are the contents of grid delineation, and 10kV trunk line wiring and branch line planning are the contents of grid planning. Among them, the load forecasting method considering load characteristics, grid division method and network frame planning method are the research focus of this paper.

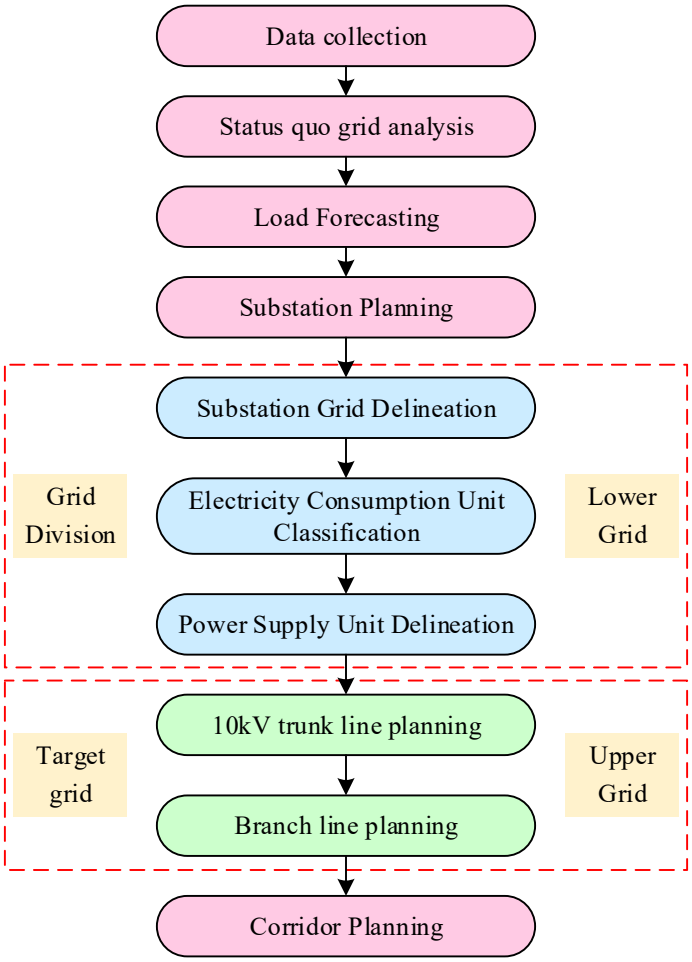

Figure 2: The grid planning process considering load characteristics

On the basis of the traditional grid planning, the grid planning process considering load characteristics analyzes the load characteristics of the planning area, applies the results of the load characteristics analysis to load forecasting and grid division, and finally carries out grid planning for the divided area. The most prominent feature is the introduction of power consumption unit, which focuses on considering the power demand of loads and reasonably utilizes the load characteristics, thus realizing the purpose of improving the utilization rate of equipments, reducing the outlet interval of substations, and reducing the investment cost.

III. Power supply meshing model under load forecasting

III. A. Load forecasting methods for built-up areas

III. A. 1) Trend extrapolation

The trend extrapolation method is suitable for medium- and long-term load forecasting with complete historical data, and is characterized by simple calculation and strong applicability. The trend extrapolation method takes the historical data of various loads as the dependent variable, and the factors related to the load data as the independent variables, establishes a mathematical model by regression analysis, and repeatedly calculates the prediction results. The commonly used mathematical functions for regression analysis are four kinds of exponential function, linear function, power function and polynomial, and their mathematical expressions are shown in equations (1)-(4).

Exponential function:

$$y = ae^{bx} \tag{1}$$

Linear functions:

$$y = ax + b \tag{2}$$

Power Functions:

$$y = ax^{b} \tag{3}$$

Polynomial:

$$y = ax^2 + bx + c \tag{4}$$

where: y is the dependent variable; a, b, c are the regression coefficients. x is the independent variable.

By analyzing the load values predicted by the regression curve model, combining the current economic development situation and the development and construction of the planning area, the results of various regression model predictions are comprehensively analyzed, and finally the load prediction results of the trend extrapolation method are obtained.

III. A. 2) Gray theory approach

Gray theoretical method makes a prediction of the future state of the system through the processing of raw data and the establishment of a gray model. At present, the $GM(1,1)$ model is more widely used, but the $GM(1,1)$ model is only applicable to a single exponential change of the sequence, which cannot reflect the development trend of the power load well. To address this problem, the gray Verhulst model can be used to predict the S-type sequence with a saturated state. In order to improve the accuracy of the prediction, the residuals of the predicted data can be corrected with a Markov model, i.e., the gray Markov Verhulst model.

Let the original sequence of the sample be $X^{(0)} = \left(x_1^{(0)}, x_2^{(0)}, \cdots, x_n^{(0)}\right)$, and the first-order cumulative addition of this sequence obtains the new data sequence as $X^{(1)} = \left(x_1^{(1)}, x_2^{(1)}, \cdots, x_n^{(1)}\right)$, where there is equation (5):

$$x_k^{(1)} = \sum_{i=1}^{k} x_i^{(0)} \quad k = 1, 2, \cdots, n \tag{5}$$

The immediate neighborhood mean generating sequence is obtained from the new cumulative sequence as $Z^{(1)} = \left(Z_1^{(1)}, Z_2^{(1)}, \cdots, Z_n^{(1)}\right)$, where Eq. (6):

$$Z_k^{(1)} = \frac{\left(x_k^{(1)} + x_{k-1}^{(1)}\right)}{2} \quad k = 2, 3, \cdots, n \tag{6}$$

The whitened differential equation for the gray Verhulst model is established as equation (7):

$$\frac{dx^1(t)}{dt} + ax^1(t) = b\left(x^1(t)\right)^2 \tag{7}$$

The parameters a, b can be obtained by least squares estimation, let $A = (a, b)^{\mathrm{T}}$ be the parameter column, then the minimum estimation of the parameter column is $A = \left(B^{\mathrm{T}}B\right)^{-1} B^{\mathrm{T}}Y$, where equation (8):

$$B = \begin{bmatrix} -Z_2^{(1)} & \left(-Z_2^{(1)}\right)^2 \\ -Z_3^{(1)} & \left(-Z_3^{(1)}\right)^2 \\ \vdots & \vdots \\ -Z_n^{(1)} & \left(-Z_n^{(1)}\right)^2 \end{bmatrix} \quad Y = \begin{bmatrix} x_2^{(0)} \\ x_3^{(0)} \\ \vdots \\ x_n^{(0)} \end{bmatrix} \tag{8}$$

The obtained a and b are brought into the whitened differential equation to obtain the time response equation for the gray Verhulst model as in equation (9).

$$\hat{x}_{k+1}^{(1)} = \frac{ax_1^{(0)}}{bx_1^{(0)} + \left(a - bx_1^{(0)}\right)e^{ak}} \tag{9}$$

The cumulative reduction of Eq. (9) yields a gray Verhulst prediction model for the original data sequence as shown in Eq. (10).

$$\hat{x}_{k+1}^{(0)} = \hat{x}_{k+1}^{(1)} - \hat{x}_k^{(1)} \tag{10}$$

The gray Verhulst model is suitable for S-growth data prediction with saturation characteristics. In practice, the gray Verhulst model only has high accuracy in the first few data, and the data predicted after that can only reflect the trend of the data. In order to cope with this problem, the Markov model is introduced into the gray Verhulst model to correct the residuals, which can effectively improve the model accuracy.

The Markov process is a discrete stochastic process with no aftereffect, and the state of the stochastic process in the "future" is only related to the state in which it is "now", but not to what state it was in in the "past".

The residual ratio between the predicted and actual values of the gray Verhulst model is divided into a number of states, each of which belongs to the range of variation of the residual ratio within the state, and the mathematical expression is shown in Equation (11).

$$Q_i \in [Q_{i1}, Q_{i2}] \quad i = 1, 2, \cdots, n \tag{11}$$

Counting the number of times state Q_i is transformed into Q_j occurrences as M_{ij} and the number of times state Q_i occurs in the sample as M_i, the probability of transforming from state Q_i to Q_j is equation (12):

$$P_{ij} = M_{ij} / M_i \tag{12}$$

This results in a state transfer probability matrix P, the expression of which is shown in Equation (13).

$$P = \begin{bmatrix} P_{11} & P_{12} & \cdots & P_{1n} \\ P_{21} & P_{22} & \cdots & P_{2n} \\ \cdots & \cdots & \cdots & \cdots \\ P_{n1} & P_{n2} & \cdots & P_{nn} \end{bmatrix} \tag{13}$$

The probability of occurrence of the predicted residual ratio in the interval of change can be obtained, and the predicted residual value can be obtained as shown in Equation (14). Finally, the obtained residual value is brought into the original prediction value for correction to improve the accuracy of prediction.

$$Q = \sum_{i=1}^{n} \frac{Q_{i1} + Q_{i2}}{2} P \tag{14}$$

III. B. Power supply unit division model

III. B. 1) Objective function

The division of power supply units of MV supply network should be based on the objective function of minimum number of power supply units, so as to improve the utilization rate of each feeder and reduce the number of substation outgoing lines by tapping the degree of matching of load characteristics between feeders. However, the planning objective of simply considering the minimum number of power supply units has a stepwise nature, and it is easy to generate multiple planning schemes with the same number of power supply units. Therefore, on the basis of meeting the minimum number of power supply units, it is also necessary to meet the balanced maximum load ratio of the transferring lines within each power supply unit in order to further judge the advantages and disadvantages of the division of power supply units. Considering the balanced maximum load factor of transfer lines as a unit of power supply unit also helps to reduce the network loss in power supply network planning. The specific objective functions are shown in Eqs. (15)-(17):

$$\min Z \tag{15}$$

$$Z = Z_{zj} + Z_{zn} \tag{16}$$

$$\min \alpha = \sum_{i=1}^{Z} \left(\eta_{i\max} - \bar{\eta}\right)^2 / Z \tag{17}$$

where Z, Z_{zj} and Z_{zn} denote the number of all, inter-station and intra-station supply units, respectively. α is the variance of the maximum load rate of the transfer lines within each power supply unit, which describes the equalization between the maximum load rates of the transfer lines within each power supply unit. $\eta_{i\max}$ denotes the maximum load rate of the transfer line in the i th power supply unit. $\bar{\eta}$ denotes the average value of the maximum load rate of the transfer lines in each power supply unit.

III. B. 2) Constraints

(1) Maximum Load Ratio Constraints for Transfer Lines in Power Supply Units

The traditional $N-1$ security constraint requires that the maximum load ratio of each feeder in the power supply network is less than the upper limit of the load ratio in the wiring mode, e.g., the maximum load ratio of each feeder in the single-contact wiring mode is 50%. Since the focus of this paper is on the power supply unit, the constraint is that the transfer line in the power supply unit is not overloaded.

For the i th power supply unit, if any one feeder line of the power supply unit is faulty, the maximum load factor of the non-faulty feeder to the faulty feeder after transferring the supply line is $\eta_{i\max}$, which is calculated as shown in Equation (18):

$$\eta_{i\max} = \frac{W_{i\max}}{L_{\max} \cdot \cos\phi} \tag{18}$$

where $W_{i\max}$ is the maximum value of the sum of the timing characteristics of the total loads in the i th supply unit, $L_{\max}$ is the maximum transmission capacity of the feeder line, and $\cos\varphi$ is the power factor. The maximum load factor of the transfer line within the supply unit is constrained as in equation (19):

$$\eta_{i\max} \le 100\% \tag{19}$$

(2) Feeder slack load rate constraints

In order to fully exploit the matching degree of load characteristics between the contact feeders, the slack load rate η_0 of each inter-station feeder is controlled with a lower limit of $k_{\min}$ and an upper limit of $k_{\max}$. The i th feeder slack load rate constraint is specified as shown in equation (20).

$$\frac{Y_{i\max}}{L_{\max}\cdot\cos\phi} \le \eta_0 \tag{20}$$

where $Y_{i\max}$ is the maximum value of the sum of the timing characteristics of the load carried by the i th feeder.

III. C. Framework for the iterative division of inter- and intra-station power supply units

Considering the division of power supply units with matching load characteristics between contact feeders, the first step is to divide the inter-station power supply units based on the method of feeder slack load rate control, and generate Nsep groups of inter-station power supply unit division schemes by changing the position of inter-station feeders for multiple iterations under each slack load rate. The average value of the load simultaneous rate in each interstation power supply unit is used as an index to evaluate the advantages and disadvantages of the interstation power supply unit division, and multiple groups of interstation power supply unit division schemes are selected. On this basis, the division of station power supply units considering the matching of load characteristics between contact feeders is carried out to form the division scheme under the slack load rate of this kind of interstation feeder. The above process is repeated by changing the slack load rate of the interstation feeder, and the interstation and intra-station power supply units are divided iteratively for many times.

IV. Evaluation and analysis of the effectiveness of the application of the model

IV. A. General overview of the zone

W District is located in the middle of the mountain range of the prefecture level city in which it is situated, and its scenic area consists of four major scenic areas with their own distinctive features. The orientation is 110°20′ ~110°41′ east longitude and 29°16′ ~29°24′ north latitude. It is a rare sandstone peak forest landscape in the world, with a total of 3103 stone peaks, the peaks are distributed at an altitude of 500~1100 meters, with heights ranging from tens of meters to 400 meters, the W area has complex topography, mild climate, abundant rainfall, lush forest development, and growth of primitive sub-forest flora. The W Scenic Spot is a national famous tourist scenic spot, with a total area of 398 square kilometers. Under the jurisdiction of four townships, of which W urban area is located in the western part of the town, with a power supply area of 5.38 square kilometers.

Typical users of residential, commercial, industrial, office and other major load types in W area are selected to analyze their load characteristics, and the load characteristic curves of different seasonal power consumption types are drawn in Fig. 3.

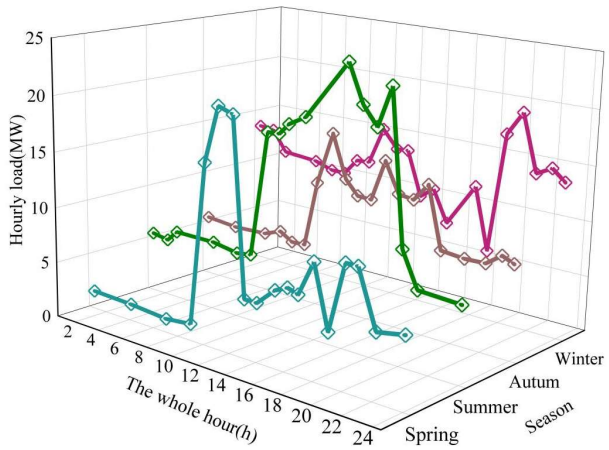

Figure 3: The typical characteristics of administrative office users in Area W

Observing Figure 3, the load characteristics of the typical day of administrative office electricity consumption in each season are characterized as follows:

(1) Except for the winter season, the main time of electricity consumption in other seasons is concentrated between 9:00 and 21:00, and there is an early peak at 10:00 and a late peak at 18:00, while in winter there is a late peak at 21:00.

(2) Comparing the typical daily load curves for the four seasons of spring, summer, fall, and winter, for the administrative office users, the season with the highest electricity load is summer and the lowest is spring.

The load characteristic curves of typical users living in W area are shown in Fig. 4.

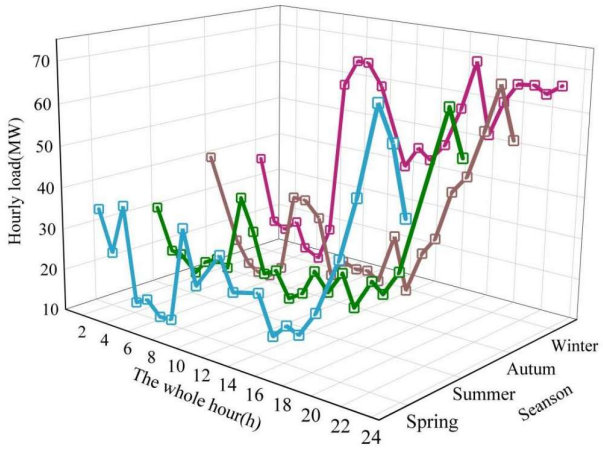

Figure 4: The load characteristics of typical residential users in Area W

The load characteristics of typical days in each season for residential electricity use are characterized as follows:

(1) For the spring, summer and fall seasons, the morning and evening peaks occur at 8:00 and 22:00 respectively. In winter, on the other hand, the load of electricity consumption is higher from 8:00 to 24:00, and sustained peaks occur from 8:00 to 11:00, 18:00, and 20:00 to 24:00.

(2) Comparing the typical daily load curves for the spring, summer, fall and winter seasons, for residential customers, the season with the highest load is winter, and the loads in spring, summer and fall are basically the same.

IV. B. Model Training and Case Analysis

In this section, the short-term forecasting model training of substation loads is carried out using the load data of W substation as a sample. In this case, the data samples are used as the load data of the substation for the month of December 2023, and the load data are sampled values every 20 minutes, totaling 2,232 sampling points for the whole month. Comparing the performance of this paper's model and the GRU model, the first 2000 conforming data are selected for grid training, the prediction input is the load data of the previous hour (3 sampling values), and the output is the load value at the current moment, and the last day's load prediction results are tested using the trained network. The statistical errors of the two models in the first 1000 tests are shown in Fig. 5.

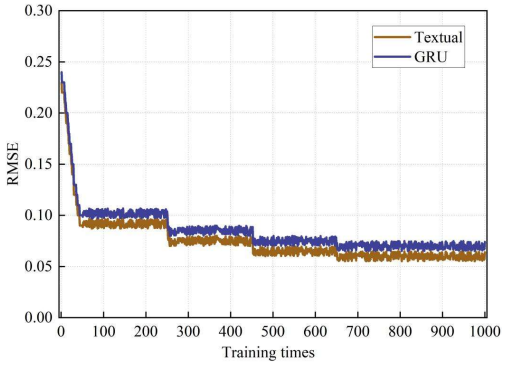

Figure 5: Model training RMSE curve

As can be seen from Fig. 5, under the same internal parameter settings of the model, although the training error trends of the two models are more consistent, the RMSE curve of the model in this paper has a faster convergence speed, and the overall training error is lower than that of the GRU model by about 0.01.

Considering that short-term load changes are easily affected by temperature, humidity and other meteorological factors, this paper collects meteorological data in the area where W substation is located, including temperature, humidity, barometric pressure and other nine types of collection. There are a total of 689 points. In addition, the change of short-term load is also related to the load characteristics of the current period, so the hourly maximum load, minimum load, and average load calculated on a rolling basis are also considered in the construction of the sample. Based on the above considerations, some of the data samples constructed are shown in Table 1, and the sampled data categories are (a) current load (MW), (b) hourly maximum load (MW), (c) hourly most average load (MW), (d) hourly minimum load (MW), (e) temperature (°C), (f) humidity (%), (g) barometric pressure (hPa), (h) surface wind speed (m/s), (i) precipitation (mm), (j) surface horizontal radiation (W/m²), (k) wind direction (°), (l) direct radiation (W/m²), (m) scattered radiation (W/m²).

Table 1: Some data samples

Type	Sampling site						
a	1	2	3	4	5	6	…
b	10.597	9.355	9.527	8.881	7.747	8.209	…
c	10.597	10.597	10.597	10.597	9.527	9.527	…
d	10.597	9.355	9.355	8.881	7.747	7.747	…
e	10.597	9.976	9.8263	9.59	8.8775	8.591	…
f	-7.2529	-7.2529	-7.2529	-7.2529	-7.1061	-7.1061	…
g	973.1775	973.1775	973.1775	973.1775	972.5319	972.5319	…
h	1.6853	1.6853	1.6853	1.6853	1.7307	1.7307	…
i	0.0000	0.0000	0.0000	0.0000	0.0000	0.0000	…
j	0.0000	0.0000	0.0000	0.0000	0.0000	0.0000	…
k	273.2304	273.2304	273.2304	273.2304	282.4519	282.4519	…
l	0.0000	0.0000	0.0000	0.0000	0.0000	0.0000	…
m	0.0000	0.0000	0.0000	0.0000	0.0000	0.0000	…

Using the power supply meshing model in this paper, the substation load curve in the W area is modally decomposed, and the change characteristics of different frequencies of the load are extracted in Fig. 6. It can be seen that after the original signal is modally decomposed, five modal components (IMF) and one residual signal (R) can be obtained. Among them, the frequency magnitude decreases gradually from IMF1 to R. The faster frequency of IMF1~3 represents the short-term trend of the load, which is susceptible to change by small perturbations. The lower frequency of IMF4~5 represents the long-term characteristics of the load in the area. R represents the long-term trend of the load, and it can be seen that, in December 2023, the local electricity consumption is gradually decreasing.

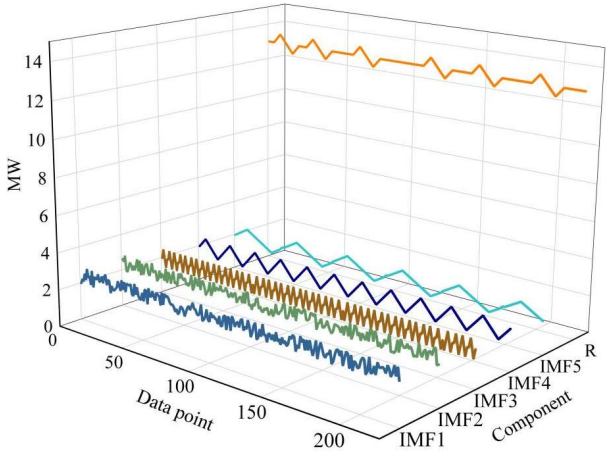

Figure 6: Modal decomposition results

IV. C. Planning effectiveness

Through the planning and construction of the power supply grid based on the model in this paper, (P1) the reliability of supply (RS-3) is improved from 99.9434% in the status quo year (2023) to 99.9955% in the target year. (P2) Average annual household outages reduced from 2.5497 (outages/household) in the status quo year to 0.83 (outages/household) in the target year. (P3) Line insulation rate increased from 75.2% in the status quo year to 100% in the target year. (P4) Line contact rate improved from 87.21% in the status year to 100% in the target year. (P5) Inter-station contact rate increased from 87.21% in the current year to 100% in the target year. (P6) “N-1” pass rate improved from 42.38% in the status year to 100% in the target year. (P7) Medium voltage line load factor average reduced from 56.55% in the status year to 48.85% in the target year. (P8) Line supply radius compliance rate increased from 90.66% in the status year to 100% in the target year. (P9) Power supply automation coverage rate increased from 5% in the status quo year to 100% in the target year.The effect of power supply grid enhancement in District W is shown in Figure 7.

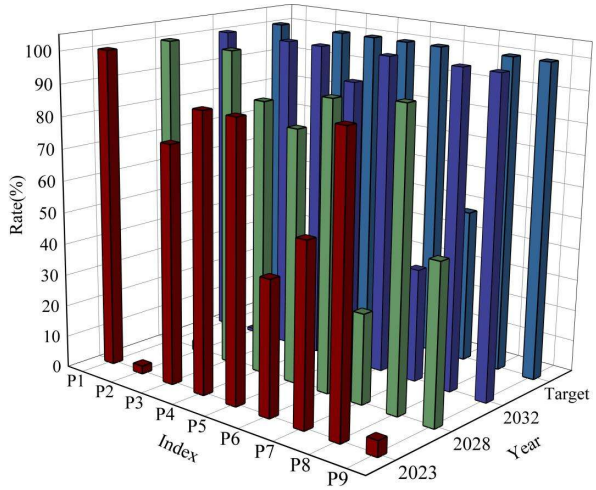

Figure 7: The improvement effect of the distribution network in Area W

V. Conclusion

In this paper, the trend extrapolation method and the gray theory method are used to predict the load trend of the power supply grid with high accuracy, which provides data reference for the planning and division of the power supply grid. At the same time, the power supply grid is combined into power supply units, and a power supply unit division model is constructed for planning, which is combined with an iterative power supply unit division framework to form a power supply grid division model. With the quantitative analysis of grid load and power supply units, the model successfully realizes the rational planning of power supply grids, which provides effective technical support for the improvement of power supply grid planning refinement level and operation efficiency. The model is used to plan the power supply grid in W area, and the training error of the model is less than 0.01 of similar models based on the power supply data in W area. Combined with the analysis of power consumption characteristics and load modes in W area, the power supply grid planned by the model in this paper is expected to increase to 100% in terms of line insulation rate, line power supply radius compliance rate, and power supply automation coverage rate.

Funding

This work was supported by Science and Technology Project of State Grid Corporation of China (5400-202318203A-1-1-ZN).

References

[1] Liu, Z., Liu, H., Xu, Z., Li, R., Guo, Y., & Du, Y. (2025). Differentiated reliability-based regional distribution network planning with probability characteristics of PV and load. IEEE Transactions on Industry Applications.

[2] Mahmud, N., & Zahedi, A. (2016). Review of control strategies for voltage regulation of the smart distribution network with high penetration of renewable distributed generation. Renewable and Sustainable Energy Reviews, 64, 582-595.

[3] Jin, B. (2023). Impact of renewable energy penetration in power systems on the optimization and operation of regional distributed energy systems. Energy, 273, 127201.

[4] Song, Y., Zheng, Y., Liu, T., Lei, S., & Hill, D. J. (2019). A new formulation of distribution network reconfiguration for reducing the voltage volatility induced by distributed generation. IEEE Transactions on Power Systems, 35(1), 496-507.

[5] Cho, Y., Lee, E., Baek, K., & Kim, J. (2023). Stochastic Optimization-Based hosting capacity estimation with volatile net load deviation in distribution grids. Applied Energy, 341, 121075.
[6] Wang, P., Yan, X., Zhao, J., Liu, P., Guo, J., Shi, H., & Tan, C. (2025). Optimization of Energy Efficiency in Low Voltage Networks Considering Variable Volatility. IEEE Access.
[7] Xing, F., Li, X., Fan, H., Zhao, K., Li, S., & Li, C. (2023). Static equivalent of distribution network with distributed PV considering correlation between fluctuation of PV and load. Frontiers in Energy Research, 10, 1119174.
[8] Panigrahi, R., Mishra, S. K., Srivastava, S. C., Srivastava, A. K., & Schulz, N. N. (2020). Grid integration of small-scale photovoltaic systems in secondary distribution network—A review. IEEE Transactions on Industry Applications, 56(3), 3178-3195.
[9] Xu, Z., Liu, H., Sun, H., Ge, S., & Wang, C. (2022). Power supply capability evaluation of distribution systems with distributed generations under differentiated reliability constraints. International Journal of Electrical Power & Energy Systems, 134, 107344.
[10] Li, Y., Du, M., Xie, W., Yang, B., Fang, C., Zhang, Y., & Wang, S. (2018). Method for division of urban load power supply district based on cluster analysis. IET Generation, Transmission & Distribution, 12(20), 4577-4581.
[11] Liu, X. (2021). Automatic routing of medium voltage distribution network based on load complementary characteristics and power supply unit division. International Journal of Electrical Power & Energy Systems, 133, 106467.
[12] Yaolei, W., Rong, L., Kuihua, W., Ren, Z., & Zhao, L. (2020, October). Construction and application of distribution network grid planning system. In Journal of Physics: Conference Series (Vol. 1659, No. 1, p. 012026). IOP Publishing.
[13] Sireesha, R., Rao, C. S., & Kumar, M. V. (2023). Graph theory based transformation of existing Distribution network into clusters of multiple micro-grids for reliability enhancement. Materials Today: Proceedings, 80, 2921-2928.
[14] Chai, Y., Guo, L., Wang, C., Zhao, Z., Du, X., & Pan, J. (2018). Network partition and voltage coordination control for distribution networks with high penetration of distributed PV units. IEEE Transactions on Power Systems, 33(3), 3396-3407.
[15] Ruan, H., Gao, H., Liu, Y., Wang, L., & Liu, J. (2020). Distributed voltage control in active distribution network considering renewable energy: A novel network partitioning method. IEEE Transactions on Power Systems, 35(6), 4220-4231.
[16] Meng, L., Yang, X., Zhu, J., Wang, X., & Meng, X. (2024). Network partition and distributed voltage coordination control strategy of active distribution network system considering photovoltaic uncertainty. Applied Energy, 362, 122846.
[17] Osama, R. A., Zobaa, A. F., & Abdelaziz, A. Y. (2019). A planning framework for optimal partitioning of distribution networks into microgrids. IEEE Systems Journal, 14(1), 916-926.
[18] Li, P., Zhang, C., Wu, Z., Xu, Y., Hu, M., & Dong, Z. (2019). Distributed adaptive robust voltage/var control with network partition in active distribution networks. IEEE Transactions on Smart Grid, 11(3), 2245-2256.